Nien-Ting Chiang, Li-Ting Ma, Yi-Ru Lee, Nai-Wen Tsao, Chih-Kai Yang, Sheng-Yang Wang and Fang-Hua Chu*

The gene expression and enzymatic activity of pinoresinol-lariciresinol reductase during wood formation in *Taiwania cryptomerioides* Hayata

https://doi.org/10.1515/hf-2018-0026
Received February 7, 2018; accepted July 13, 2018; previously published online August 14, 2018

Abstract: Taiwania (*Taiwania cryptomerioides* Hayata) is an indigenous conifer species of Taiwan. Various secondary metabolites of Taiwania with diverse bioactivities have been identified, and lignans are especially abundant in the heartwood (hW). In the present study, the wood of this species was separated to cambium (Cam), sapwood (sW), transition zone (TZ) and hW and their transcriptomes were sequenced. Three pinoresinol-lariciresinol reductases (*PLR*s; designated *TcPLR1*, *TcPLR2.2* and *TcPLR3*), which are responsible for lignan biosynthesis, were cloned and their expressions in wood tissues were detected. *TcPLR*s had higher expression levels in Cam and sW in RNA-seq and reverse transcriptase-polymerase chain reaction (RT-PCR) results. Liquid chromatography-mass spectrometry (LC-MS) analysis of the reaction products of TcPLRs revealed that TcPLR1 can reduce (+)-pinoresinol to lariciresinol, and both TcPLR2.2 and TcPLR3 could reduce (+)-pinoresinol to lariciresinol and secoisolariciresinol.

Keywords: Cupressaceae, lignin, pinoresinol-lariciresinol reductase, *Taiwania cryptomerioides* Hayata, wood transcriptome

***Corresponding author: Fang-Hua Chu,** School of Forestry and Resource Conservation, National Taiwan University, Taipei 10617, Taiwan; and Experimental Forest, National Taiwan University, Nantou 55750, Taiwan, Phone: +886-2-33665261, Fax: +886-2-23654520, e-mail: fhchu@ntu.edu.tw
Nien-Ting Chiang, Li-Ting Ma and Yi-Ru Lee: School of Forestry and Resource Conservation, National Taiwan University, Taipei 10617, Taiwan
Nai-Wen Tsao: Department of Forestry, National Chung-Hsing University, Taichung 40227, Taiwan
Chih-Kai Yang: Experimental Forest, National Taiwan University, Nantou 55750, Taiwan
Sheng-Yang Wang: Department of Forestry, National Chung-Hsing University, Taichung 40227, Taiwan; and Agricultural Biotechnology Research Center, Academia Sinica, Taipei 11529, Taiwan

Introduction

Lignans are phenylpropanoids formed from two phenylpropanes dimerizing at the 8-8′ site and they are supposed to protect plants from abiotic and biotic stresses (Vassão et al. 2010). The way of dimerization determines their chiral properties (Suzuki and Umezawa 2007). Lignans are widespread in plant families, and their composition and their enantiomers ratios vary with plant species and even within various tissues (Suzuki et al. 2002; Hemmati et al. 2010; Vassão et al. 2010). Because of their biological activities toward insects, such as antifeedant activities, molting disturbances, growth inhibition and mortality, they are potential insecticides (Harmatha and Dinan 2003; Saguez et al. 2013). Lignans also show antifungal, antimicrobial and antioxidant activities (MacRae and Towers 1984; Larson 1988; Fauré et al. 1990; Vargas-Arispuro et al. 2005). In wood, lignans are responsible for the unique color and durability of the heartwood (hW) (Chang et al. 1999; Johansson et al. 2000; Suzuki and Umezawa 2007). Lignans are also present in the sapwood (sW) after a fungal attack, and this emphasizes their role as defense against fungal pathogens (Kemp and Burden 1986). A relationship between the lignan biosynthetic gene, *pinoresinol reductase 1 of Arabidopsis* (*AtPrR1)*, and secondary cell wall formation was also reported (Zhao et al. 2015). Lignans are known to have several bioactivities in human healthcare and show antioxidative, anti-inflammatory and anticancer activities (Adlercreutz 2007; Vassão et al. 2010; Satake et al. 2015).

The biosynthesis of upstream lignans including pinoresinol, lariciresinol, secoisolariciresinol and matairesinol are described for several plant species as illustrated in Figure 1 (Suzuki and Umezawa 2007; Satake et al. 2015). Lignin and lignan share the same biosynthetic pathway from phenylalanine to coniferyl alcohol (CA) (Vanholme et al. 2010). CA can be oxidized by laccase, peroxidase or other single-electron oxidant, and the dimerization of two CA radicals at 8-8′ generates the lignan pinoresinol (Suzuki and Umezawa 2007; Vassão et al. 2010). This dimerization is mediated by

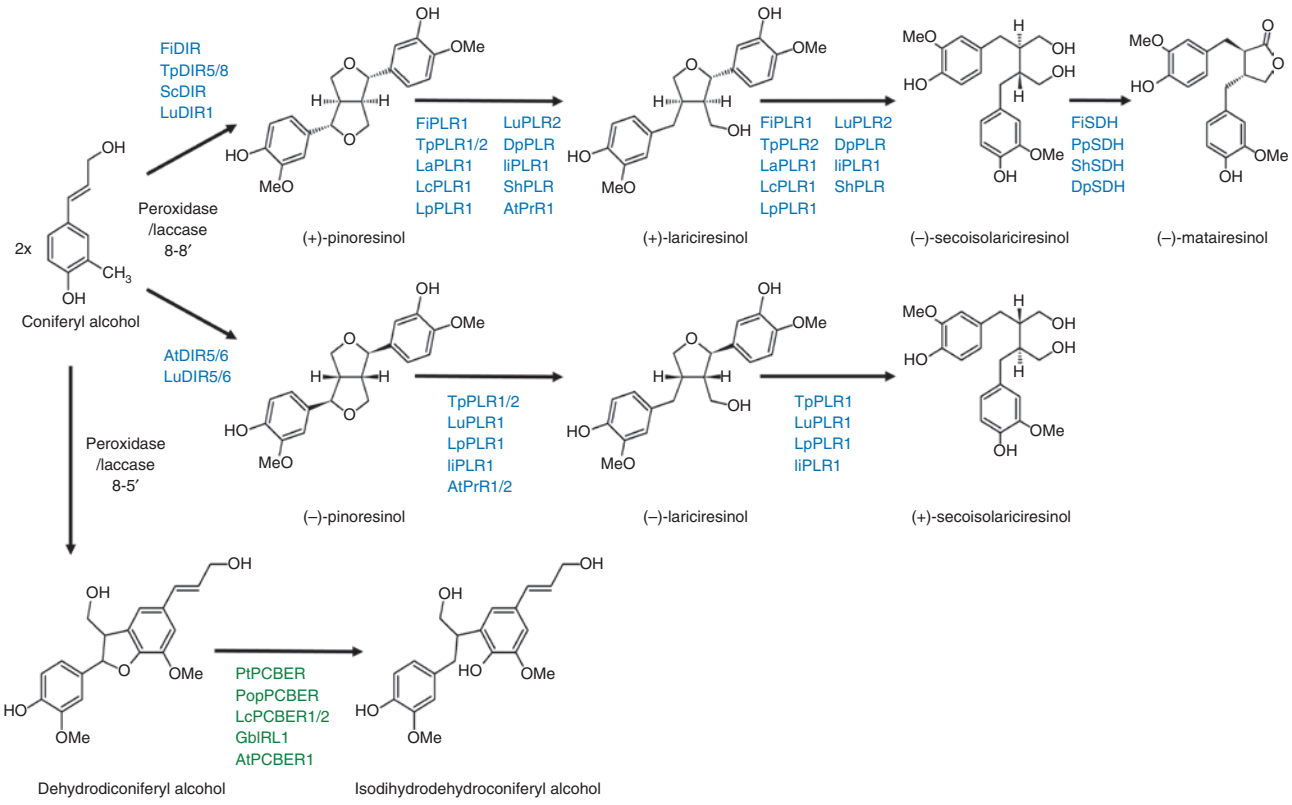

Figure 1: General biosynthetic pathway of lignans and neolignans.
Blue, lignan biosynthetic enzymes; Green: neolignan biosynthetic enzymes. The abbreviations of plant species are as follows: At, *Arabidopsis thaliana* (L.) Heynh.; Dp, *Dysosma pleiantha* (Hance) Woodson; Fi, *Forsythia x intermedia* Zabel; Gb, *Ginkgo biloba* L.; Ii, *Isatis indigotica* Fortune; La, *Linum album* Kotschy ex Boiss.; Lc, *Linum corymbulosum* Rchb.; Lp, *Linum perenne* L.; Lu, *Linum usitatissimum* L.; Pt, *Pinus taeda* L.; Pp, *Podophyllum peltatum* L., 1753; Pop, *Populus trichocarpa* Torr. & A. Gray; Sc, *Schisandra chinensis* (Turcz.) Baill.; Sh, *Sinopodophyllum hexandrum* (Royle) T.S. Ying; Tp, *Thuja plicata* Donn ex D. Don (Dinkova-Kostova et al. 1996; Fujita et al. 1999; Gang et al. 1999a,b; Xia et al. 2001; Kim et al. 2002, 2012; von Heimendahl et al. 2005; Hemmati et al. 2007, 2010; Bayindir et al. 2008; Nakatsubo et al. 2008; Vassão et al. 2010; Cheng et al. 2013; Kuo et al. 2014; Niculaes et al. 2014; Dalisay et al. 2015; Lau and Sattely 2015; Xiao et al. 2015; Nuoendagula et al. 2016).

dirigent proteins (DPs), which lead to the production of (+)-pinoresinol or (–)-pinoresinol (Gang et al. 1999a; Kim et al. 2002, 2012; Dalisay et al. 2015). Pinoresinol can be subsequently reduced to lariciresinol and then to secoisolariciresinol by pinoresinol-lariciresinol reductase (PLR). Secoisolariciresinol can be oxidized to matairesinol by secoisolariciresinol dehydrogenase (SDH), which was observed in *Forsythia x intermedia*, *Podophyllum peltatum*, *Sinopodophyllum hexandrum* and *Dysosma pleiantha* (Xia et al. 2001; Kuo et al. 2014; Lau and Sattely 2015). The biosynthesis of lignans downstream from matairesinol, such as hinokinin and yatein, is not fully characterized. In the case of podophyllotoxin (used for anticancer drug production), the following biosynthetic steps are known to involve methyltransferases, cytochrome P450s and a 2-oxoglutarate/Fe(II)-dependent dioxygenase (Lau and Sattely 2015).

PLR, which is the best studied lignan biosynthetic enzyme, plays a key role in determining lignan biosynthesis of the phenylpropanoid pathway. In *PLR*-silenced hairy root lines of *Linum corymbulosum*, severe reduction steps of hinokinin were observed (Bayindir et al. 2008). Also in leaves of *Linum usitatissimum*, silence of *PLR* causes significant reduction of yatein production (Corbin et al. 2017). The sequences of PLRs are similar to phenylcoumaran benzylic ether reductases (PCBERs) and isoflavone reductases (IFRs), and the enantio-specific PLRs and IFRs were hypothesized to evolve from the regio-specific PCBERs (Gang et al. 1999b). Functional characterization of PCBERs have been reported in gymnosperms and angiosperms (Gang et al. 1999b; Bayindir et al. 2008; Cheng et al. 2013; Niculaes et al. 2014; Nuoendagula et al. 2016), while IFRs have been reported in angiosperms (Paiva et al. 1991, 1994; Tiemann et al. 1991; Cheng et al. 2015). The enantio-specificities of PLRs were observed in many plant species (Figure 1). Some of the PLRs possess the same enantio-specificity, whereas PLRs with different or no enantio-specificity are also reported. For example,

the gymnosperm PLRs, TpPLR1 and TpPLR2 from western red cedar (*Thuja plicata*), can reduce both of the pinoresinol enantiomers, while selectively reduce (–)-lariciresinol or (+)-lariciresinol (Dinkova-Kostova et al. 1996; Fujita et al. 1999; von Heimendahl et al. 2005; Hemmati et al. 2007, 2010; Bayindir et al. 2008; Kuo et al. 2014; Lau and Sattely 2015; Xiao et al. 2015).

Taiwania (*Taiwania cryptomerioides* Hayata) is a monotypic conifer species of the genus *Taiwania* diverging early in the Cupressaceae family. Taiwania is a relict from the Tertiary period and is widespread in East Asia, with the main populations in Taiwan, northern Vietnam and the border area of Yunnan and Myanmar (Chou et al. 2011; Pittermann et al. 2012). To date, more than 500 secondary metabolites have been isolated from Taiwania, including lignans, terpenoids, steroids and flavonoids. Several of the metabolites are reported to have antibacterial, antifungal, antimite, antitermite and/or antitumor activities (Chang et al. 2000, 2003; Chien and Kuo 2009; Tsao et al. 2016). Lignans, which are the dominant constituents along with terpenoids of hW extractives (Chang et al. 2000; Tsao et al. 2016), contribute to the yellowish-red color hW. Several lignans identified from hW extractives exhibit antitumor activities (Chang et al. 2000). Among the lignans tested, taiwanin A showed the highest cytotoxicity by inducing apoptosis (Chang et al. 2000; Ho et al. 2007; Shyur et al. 2010; Harn et al. 2014).

The presence of lignans formed from secondary reactions (oxidation or hydrolysis) in sW distinguished the hW formation in Taiwania from the known hW formation types, and is called "Taiwania-type" hW formation (Magel 2000; Tsao et al. 2016). In the wood of Taiwania, most of the dibenzylbutyrolactone type and arylnaphthalide type lignans appear in the sW, accumulate largely in the transition zone (TZ) and reach their highest accumulation degree in the outer hW. An exception is taiwanin A, which is absent in sW and starts to accumulate in the TZ. Considering the unique structure of taiwanin A compared to lignans found in other species, it has been proposed that a specific dehydrogenase would be responsible for its biosynthesis from savinin or hinokinin (Tsao et al. 2016). Nevertheless, no lignan biosynthetic enzyme has been found in Taiwania so far. It was demonstrated that in sandalwood (*Santalum album* L.) a cytochrome P450 which catalyzed the last biosynthetic steps of fragrant sesquiterpenoids has the hW-specific expression pattern that matches the distribution of fragrant sesquiterpenoids (Celedon et al. 2016). Together with lignan distribution reported previously, the information of gene expression in wood would be helpful to study lignan biosynthesis, and its relation to the unique process of hW formation in Taiwania.

In this study, the transcriptome of wood in various development stages – cambium (Cam), sW, TZ and hW – was sequenced separately for gene expression analysis with respect to lignan distribution. The biosynthetic pathway genes should be identified, and their expression should be quantified by the RNA-Seq strategy. There will be a focus on the key enzymes TcPLRs (named TcPLR1~3). The principal goal of the study is to elucidate the question of how gene expression governs upstream lignan biosynthesis.

Materials and methods

Plant material: The Taiwania tree was 30 years old (20 m height) and grown in the Huisun Experimental Forest Station of National Chung Hsing University. The sample trunk was 1.6 m above the ground, and 34 cm in diameter and 11 cm in height. The bark was removed first, and the thin, pinkish layer Cam outside the sW was scraped with a blade. The sW beside the Cam was collected with a rasp, and the inner sW was removed and discarded. The thin layer outside the hW (TZ), with apparently darker color compared to sW and hW, and the hW beside TZ was also collected separately with a rasp. For sampling regions of each wood tissue, refer to Figure S1. Each of the wood samples was divided into small pieces, mixed and frozen with liquid nitrogen immediately after separation and stored at –80°C before total RNA isolation.

For the positive control of the PLR activity assay, DpPLR from *D. pleiantha* was chosen because of the accessibility of plant material in Taiwan. Leaves of *D. pleiantha* were harvested in the Highland Experimental Farm of National Taiwan University. Leaves without petioles were broken into small pieces, mixed together in liquid nitrogen and stored at –80°C before total RNA isolation.

RNA isolation: The total RNA of Cam was extracted according to Chang et al. (1993). However, in order to eliminate the interfering materials, the total RNA of sW, TZ and hW were extracted according to Bugos et al. (1995) and modified as described by Yoshida et al. (2007). Approximately 4 g, 9 g, 33 g and 107 g samples of Cam, sW, TZ and hW, respectively, were used to isolate total RNA for transcriptome sequencing and the following experiment. Genomic DNA was removed using Plant Total RNA Miniprep Purification Kit (GeneMark, Taichung, Taiwan) and DNase I (Fermantas, Vilnius, Lithuania) according to the manufacturer's manual.

The total RNA of *D. pleiantha* was isolated with Plant Total RNA Miniprep Purification Kit (GeneMark) according to the manufacturer's manual, and genomic DNA was removed using DNase I (ZGene Biotech Inc., Taipei, Taiwan) and then stored at –80°C before synthesis of complementary DNA (cDNA).

Transcriptome assembly and annotation: Quality control of total RNA was determined using Agilent 2100 bioanalyzer (Agilent Technologies, Santa Clara, CA, USA), and 20 μg total RNA with higher 28S:18S ratio of each sample was sent to Beijing Genomics Institute (Shenzhen, Guangdong, China) for cDNA library construction and sequencing using Illumina Hiseq2000 platform (Illumina, San Diego, CA, USA). The accession numbers of RNA-Seq data of Cam, sW, TZ and hW are SAMN08365288, SAMN08365289, SAMN08365290 and SAMN08365291, respectively.

Transcriptome assembly and annotation were conducted using tools built in ContigViews web server (National Taiwan University, Taipei, Taiwan) (http://www.contigviews.csbb.ntu.edu.tw). For the completeness of the contigs assembled, the RNA-Seq data of Cam, sW, TZ and hW were assembled together with the RNA-Seq data of needle, male/female strobili and mixture of secondary phloem and xylem (unpublished data). Paired-end reads were first trimmed with Trimmomatic (Bolger et al. 2014) to remove low quality bases and next assembled using Trinity (Grabherr et al. 2011). The abundance of contigs were quantified using eXpress (Roberts and Pachter 2013), and the expression values were exported from ContigViews web server for further analysis. The tot_count of the eXpress result was normalized by the size factors of seven tissues using DESeq2 (Love et al. 2014) conducted in R version 3.2.0 (R Core Team, Vienna, Austria) (https://www.r-project.org). Gene annotation with coding sequence (CDS) databases of The Arabidopsis Information Resource (TAIR) and European Molecular Biology Laboratory (EMBL) were performed using the rule-based predictor, and GO enrichment analyses were performed using Blast2GO as described in Liu et al. (2014).

Identification of lignan biosynthetic pathway genes: The common phenylpropanoid and monolignol biosynthetic pathway enzymes listed in the Kyoto Encyclopedia of Genes and Genomes (KEGG) reference pathway of phenylpropanoid biosynthesis formed the basis for the search orthologs against the transcriptome library by the tblastn tool in ContigViews web server. The e-values were set less than 1×10^{-100}. To identify lignan biosynthetic genes, TpDP3 and TpPLR2 from *T. plicata* were used as queries for the tblastn search and the e-values were set less than 1×10^{-50}. The corresponding genes were named *TcDP1* and *TcPLR1~3*, respectively, with a number after decimal point indicating transcript isoforms.

Sequence alignments and phylogenetic tree construction: The sequence of *TcPLR*s were translated by the ExPASy translate tool (SIB Swiss Institute of Bioinformatics, Lausanne, Vaud, Switzerland) (http://web.expasy.org/translate) and then searched against the National Center for Biotechnology Information (NCBI) Conserved Domain Database (CDD) for identification of conserved domains. For sequence alignments of TcPLRs with other PLRs, the CLC Sequence Viewer 7 (QIAGEN, Hilden, NRW, Germany) (https://www.qiagenbioinformatics.com) was used to present the alignment results. For phylogenetic tree construction, the amino acid sequences of PLRs, PCBERs and IFRs were aligned using ClustalW built in Molecular Evolutionary Genetics Analysis Version 6.0 (MEGA 6.0) (Tamura et al. 2013). The phylogenetic tree was next generated based on the alignment result using the neighbor-joining method. Phylogeny was tested using the bootstrap method and the number of replications was 1000. Other parameters were set as default.

Detection of *TcPLR*s in wood tissues: The expression levels of *TcPLR*s in Cam, sW, TZ and hW were further examined by reverse transcriptase polymerase chain reaction (RT-PCR). For each tissue, one microgram of total RNA was used to synthesize cDNA by SuperScript IV Reverse Transcriptase (Invitrogen, Carlsbad, CA, USA). Polymerase chain reaction (PCR) of 18S ribosomal RNA gene and *TcPLR*s fragments were conducted by 2× PCR master mix (ZGene Biotech Inc.), cDNA of each wood tissue and gene-specific primers are listed in Table S1. The 18S ribosomal RNA gene served as the internal control.

Cloning of *PLR*: Synthesis of cDNA libraries of Cam, sW, TZ and hW tissue was done via SuperScript III Reverse Transcriptase (Invitrogen). cDNA was synthetized from 1 μg of total RNA of sW and TZ according to the manufacturer's manual. Hybrid RNA was removed by RNase H (Thermo Fisher Scientific Inc., Waltham, MA, USA). Primers of *TcPLR1*, *TcPLR2.2* and *TcPLR3* were designed based on the coding region of contigs. The partial coding region and the untranslated region of each *TcPLR* were amplified using 5′ and 3′ RACE system (Invitrogen) and Blend-Taq Plus (TOYOBO Co., Osaka, Japan). The complete coding region of each *TcPLR* was amplified using Phanta Super-Fidelity DNA polymerase (ZGene Biotech Inc.). The amplified DNA fragments were separated by agarose gel electrophoresis, purified with GEL/PCR Purification Kit (Favorgen Biotech Corp., Ping-Tung, Taiwan). For Sanger sequencing, amplicons were ligated into pGEM-T easy vector by T4 DNA ligase (Promega Corp., Fitchburg, WI, USA). Primers used for the cloning of *TcPLR*s are listed in Table S1.

To confirm the condition of the enzyme assay, the functionally characterized DpPLR was chosen as the positive control. Synthesis of cDNA library of *D. pleiantha* leaf tissue was done via HiScript II Reverse Transcriptase (ZGene Biotech Inc.). cDNA was synthetized from 1 μg total RNA according to the manufacturer's manual. Hybrid RNA was removed by RNase H (Thermo Fisher Scientific Inc.). Primers of *DpPLR* were designed based on the sequence (GenBank accession number: KJ000045.1) published by Kuo et al. (2014) and are listed in Table S1. The construction of *DpPLR* expression vector (designated as DpPLR-pET28) was conducted as described for *TcPLR*s.

Heterologous expression of TcPLRs: For construction of the recombinant protein expression vector, primers that contained restriction sites at 5′ end were designed to amplify the coding region of each *TcPLR* and the purified amplicons were digested by the corresponding restriction enzymes (New England Biolabs, Ipswich, MA, USA). *TcPLR*s were ligated into pET-28a(+) (Novagen, Merk Bioscience, Darmstadt, Germany) digested with the same restriction enzyme (designated as TcPLR-pET28). After verifying the coding regions of *TcPLR*s constructed in pET-28a(+) by Sanger sequencing, the recombinant TcPLRs with N- and C-terminal six histidine tag (designated as TcPLR-His × 6) were expressed in the *Escherichia coli* strain C41 (DE3) (New England Biolabs). Primers used for the cloning of *TcPLR*s are listed in Table S1.

The *Escherichia coli* strain C41 transformed with TcPLR-pET28, DpPLR-pET28 and pET-28a(+) were cultured in 5 ml Luria-Bertani (LB) broth using 50 μg ml^{-1} kanamycin (Bio Basic Ink., Markham, Ontario, Canada) for selection. The transformed cells were incubated at 37°C with vigorous shaking. After overnight incubation, 100 μl of the cell culture were added to 20 ml LB broth (containing 50 μg ml^{-1} kanamycin) and incubated under the same conditions until the OD600 reached 0.5~0.7. Expression of the recombinant protein was induced with 0.4 mM isopropyl β-D-1-thiogalactopyranoside (IPTG) (Sigma-Aldrich Corp., St. Louis, MO, USA) and incubated at 16°C for 20~22 h with shaking. Cells were collected by centrifugation at 4°C the next day and were stored at –20°C or used immediately. For Western blot analysis, cells of 5 ml culture were resuspended with 300 μl phosphate-buffered saline (PBS) buffer and lysed via sonication. The cell lysates were centrifuged at 4°C and 20 μl supernatant were transferred into new microcentrifuge tubes and mixed with protein loading dye. The mixture were boiled for 5 min, cooled on ice and used for electrophoresis of sodium dodecyl sulfate polyacrylamide gel (SDS-PAGE). The protein was transferred onto polyvinylidene

difluoride (PVDF) (Merk Millipore, Burlington, MA, USA) membrane and incubated with anti-His_6 (Roche, Basel, Switzerland) with gentle shaking. After 1 h incubation, the membranes were washed and incubated with anti-mouse (Promega Corp.) with gentle shaking for 30 min. The His-tagged recombinant proteins were detected with 5-bromo-4-chloro-3-indolyl-phosphate/nitro blue tetrazolium (BCIP/NBT) (Sigma-Aldrich Corp., St. Louis, MO, USA).

***In vitro* enzyme assay and LC-MS analysis:** PLR enzyme assays and Liquid chromatography-mass spectrometry (LC-MS) were conducted according to Kuo et al. (2014) and Hemmati et al. (2007) with some adjustments. The cells which expressed TcPLRs were resuspended with 300 µl KPi buffer (0.1 M, pH 7.1) and lysed by sonication. Cell lysates were centrifuged at 4°C and then 235 µl supernatant (crude protein) was added for enzyme assays. The reaction mixture included 235 µl crude protein, 2.5 µl 20 mM pinoresinol (Sigma-Aldrich Corp.) dissolved in methanol and 12.5 µl 50 mM nicotinamide adenine dinucleotide phosphate (NADPH) (Sigma-Aldrich Corp.) dissolved in ddH_2O. The mixture of crude protein and substrate were incubated at 30°C with shaking for 15 min before NADPH was added. Then, the reaction mixture was incubated for another 3 h. The reactions were stopped by adding an eaqual volume of ethyl acetate (Echo Chemical Co., Tianhe, Guangzhou, P. R. China), and the reaction mixture was centrifuged for 5 min at 13 800 *g*. The upper organic phase was transferred to a new microcentrifuge tube and then the aqueous phase was extracted again. The combined organic phase was dried with nitrogen flow and dissolved in 50 µl acetonitrile. One microliter of the extract was analyzed by LC-MS (Dionex UltiMate 3000 UPLC, Thermo Fisher Scientific Inc.). The column was Luna 5 µm C18 column (250 × 4.6 mm) (Phenomenex, Torrance, CA, USA). The binary mobile phase consisted of 0.01% phosphoric acid (solution A) and acetonitrile (ACN) (solution B), and the gradient of the mobile phase was set as described by Kuo et al. (2014). The flow speed was 1 ml min^{-1}. The detector was set at 254 nm. The reaction products of TcPLRs were identified by comparing their retention time and mass spectra with authentic standards of (+)-lariciresinol and (±)-secoisolariciresinol (Sigma-Aldrich Corp.).

The crude protein of *E. coli* C41 (DE3) transformed with pET-28a(+) served as the negative control in enzyme assays. The crude protein of *E. coli* C41 (DE3) cells expressing DpPLR were also used in enzyme assays as a positive control. The reaction products of the positive and negative controls were analyzed with Agilent 1200 Series HPLC System (Agilent Technologies). The column and analysis conditions were the same as described earlier. The reaction products were identified by comparing the retention time with authentic standards of (+)-lariciresinol and (±)-secoisolariciresinol (Sigma-Aldrich Corp.).

Results and discussion

Construction of the Taiwania2 transcriptome database

De novo assembly of RNA-Seq data generated 223 300 contigs. The N50 of assembled contigs was 873 nucleotides, and 64 324 contigs were above 500 nucleotides long as shown in Tables S2 and S3. After comparing with the TAIR and EMBL CDS databases, 57 688 contigs (26%) were annotated, with 15 543 contigs (7%) predicted to contain full-length open reading frame (ORF) and classified as "Complete", 30 811 contigs (14%) predicted to have partial ORF and classified as "Partial" and 11 334 contigs (5%) without ORF defined and classified as "others". The remaining 74% contigs did not have homologs in TAIR/EMBL CDS databases and were thus classified as "Non-hit" (Figure S2). The alignment results of complete contigs and reference genes are presented in Figure S2.

Lignan biosynthetic pathway genes in Taiwania2 database

The tblastn results of lignan biosynthetic pathway genes are shown in Table S4. In brief, totally 49 contigs were obtained, and the encoded proteins have above 60% identities to queries, with a few exceptions. Tblastn was also performed to search *SDH* orthologs in Taiwania, and the highest identities of encoded proteins to FiSDH were 52%. As lignan and lignin share the common precursor – CA, we focused on the lignan biosynthesis branch and the functions of the three *TcPLR*s were further analyzed. *TcPLR2.2* was chosen among the other isoforms for its higher translated amino acid sequence identity to TpPLR2 (Table S4).

Expression profile of phenylrpopanoid and monolignol biosynthetic pathway genes

The expression of phenylpropanoid and monolignol biosynthetic pathway genes showed different patterns across Cam to hW. Most of pathway genes had highest expression values in sW in the RNA-seq result (Figure 2). These included genes of phenylalanine ammonia-lyase (*PAL*), cinnamate 4-hydroxylase (*C4H*), 4-coumarate:CoA ligase (*4CL*), *p*-hydroxycinnamoyl-CoA: quinate/shikimate *p*-hydroxycinnamoyl-transferase (*HCT*), *p*-coumarate 3-hydorxylase (*C3H*), Caffeoyl-CoA *O*-methyltransferase (*CCoAOMT*), cinnamoyl-CoA reductase (*CCR*) and cinnamyl alcohol dehydrogenase (*CAD*) (Figure 2 and Table S4). The expression of CA biosynthesis genes in sW could contribute to the lignan formation, and also the lignification of ray parenchyma cells (Bergstrom 2003; Zheng et al. 2014). Some of the pathway genes, such as *TcPAL3~5*, *Tc4CL2*, *TcHCT1* and *TcCAD4*, had the highest expression values in Cam. There were also several genes having higher expression values in TZ and hW, such as *TcPAL2*, *Tc4CL3*, *TcCCoAOMT2*, *TcCCR3, TcCCR4* and *TcCAD3*. The overall expression profile of phenylpropanoid and

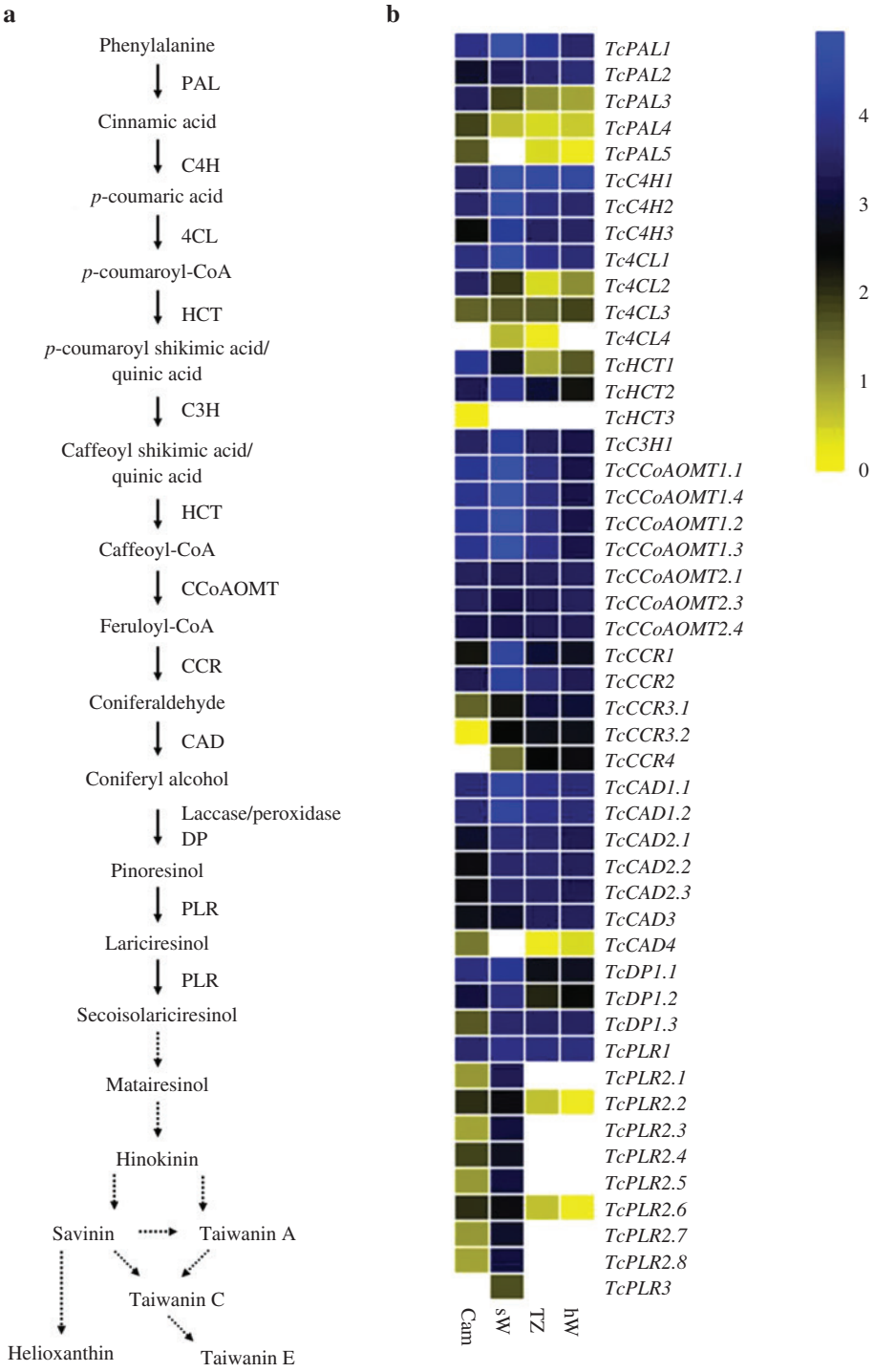

Figure 2: Expression profiling of lignan biosynthetic pathway genes using RNA-Seq.
(a) Common phenylpropanoid, monolignol and lignan biosynthetic pathways. The solid arrows are reactions catalyzed by known enzymes (bold), whereas the dashed arrows are the predicted lignan biosynthetic steps in Taiwania. (b) Expression levels of pathway genes. Expression values are presented as the base 10 logarithm of counts normalized by DESeq2. Gray box means no signal detected in RNA-Seq. The numbers after decimal point are transcript isoforms of the gene. Cam, Cambium; sW, sapwood; TZ, transition zone; hW, heartwood; 4CL, 4-coumarate:CoA ligase; C3H, *p*-coumarate 3-hydorxylase; C4H, cinnamate 4-hydroxylase; CAD, cinnamyl alcohol dehydrogenase; CCoAOMT, caffeoyl-CoA *O*-methyltransferase; CCR, cinnamoyl-CoA reductase; DP, dirigent protein; HCT, *p*-hydroxycinnamoyl-CoA: quinate/shikimate *p*-hydroxycinnamoyl-transferase; PAL, phenylalanine ammonia-lyase; PLR, pinoresinol-lariciresinol reductase; SDH, secoisolariciresinol dehydrogenase.

monolignol pathway genes revealed that precursors of lignans are biosynthesized largely in sW, and in Cam, TZ and hW as well.

The upstream phenylpropanoid and monolignol pathway genes may contribute differently to lignan biosynthesis. In the study of Chinese traditional medicine *Isatis indigotica*, only the time-course expression of *IiPAL*, *Ii4CL*, *IiC4H* and *IiC3H* correlated highly with the laricireisnol production under methyl jasmonate (MeJA) treatments (Chen et al. 2015). In Taiwania, Tsao et al. (2016) reported that lignans reached their highest accumulation in hW. The upstream pathway genes which had the highest expression levels in TZ and hW may play an important role in lignan biosynthesis.

Lignan biosynthesis in Taiwania

The results of RNA-seq and RT-PCR showed that the expression levels of lignan biosynthetic genes, *TcDP1* and *TcPLR*s, were higher in Cam and sW (Figures 2 and S3). This is consistent with most of the upstream genes, which also had higher expression values in Cam and sW. The results indicate that lignan and monolignol biosynthetic pathways are more active in Cam and sW, while the lignan content are higher in TZ and hW of Taiwania. Recently, the location of biosynthesis of hW extractives was reported for Scots pine (Pinus sylvestris L.) (Lim et al. 2016). The expression of pathway genes indicate that the phenolic compounds, stilbenes, are biosynthesized *in situ* in TZ, while resin acids are biosynthesized in sW and are transported inwards to TZ. In Taiwania, it seems that lignans are not biosynthesized simultaneously. It seems reasonable that most of the lignans identified, except for taiwanin A, are largely biosynthesized in Cam and sW, and are later transported to TZ and hW. It is also possible that lignans are biosynthesized in TZ and hW because the expression of *TcDP1* and *TcPLR1* could be detected. The absence of taiwanin A in sW (Tsao et al. 2016) can be interpreted as being biosynthesized *in situ* in TZ. The possible precursors (savinin or hinokinin) of taiwanin A could be transported from sW, or biosynthesized also in TZ.

hW extractives are thought to be biosynthesized in ray parenchyma cells in sW (Magel 2000; Nakaba et al. 2016). The detection of DP transcripts of western red cedar by *in situ* mRNA hybridization revealed that DP genes expressed in the vascular Cam and ray parenchyma cells of sW (Patten et al. 2008). Based on the same techniques, the DP transcripts and PLR transcripts of *F. x intermedia* were detected in stem vascular Cam and radial parenchyma cells (Burlat et al. 2001; Kwon et al. 2001). This is indicative of a lignan biosynthesis in vascular Cam and ray parenchyma cells of sW. Our gene expression results also support the biosynthesis of lignans in Cam and sW. In the study of Nakaba et al. (2016) on *Cryptomeria japonica* (Thunb. ex L.f.) D. Don, a hW norlignan was found to be biosynthesized in ray parenchyma cells in sW before cell death. The formation of taiwanin A, unlike other lignans found in sW in Taiwania, may take place in TZ before the programmed cell death of ray parenchyma cells.

Expression of *TcDP1* and *TcPLR*s in Cam and sW suggested the location of upstream lignan formation, although the reaction products of TcPLRs had not been reported in the wood of Taiwania. The absence of the lignan upstream of matairesinol was also typical for other species, and may be due to the rapid conversion of pinoresinol down to matairesinol (Hemmati et al. 2007).

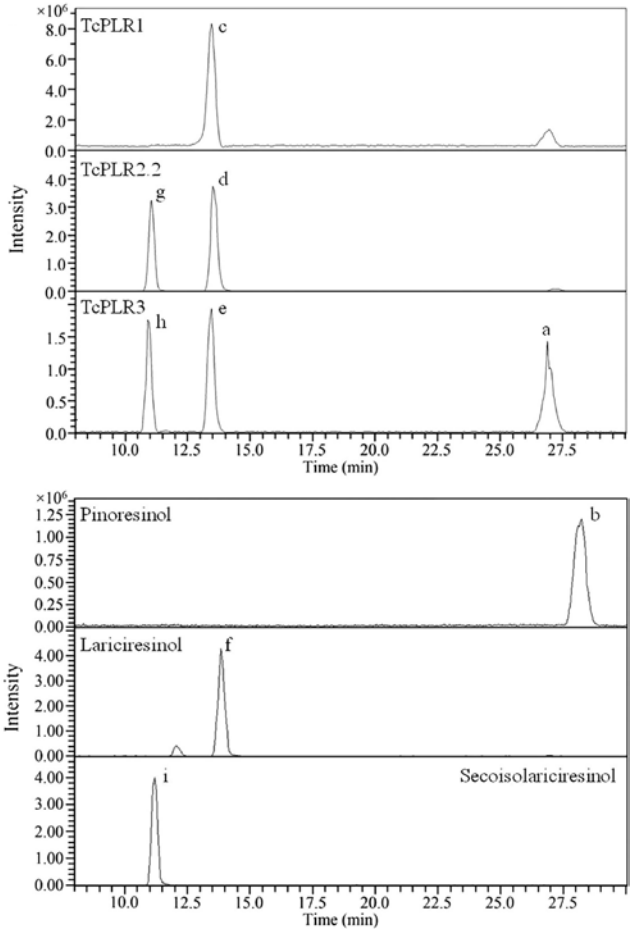

Figure 3: Identification of the products of TcPLRs.
From the top are LC profiles of TcPLR1 reaction extract, followed by TcPLR2.2 reaction extract, TcPLR3 reaction extract, (+)-pinoresinol authentic standard (Sigma-Aldrich Corp.), (+)-lariciresinol authentic standard (Sigma-Aldrich Corp.) and (±)-secoisolariciresinol authentic standard (Sigma-Aldrich Corp.). The corresponding mass spectra of peaks (labeled a~i) in LC profiles are presented in Figure S5.

The gene information provided by wood transcriptomes of different stages would be helpful in characterizing other enzymes responsible for downstream lignan biosynthesis and understanding the relationship between lignan biosynthesis and wood formation in Taiwania.

Sequence analysis and functional characterization of TcPLRs

The ORFs of *TcPLR1*, *TcPLR2.2* and *TcPLR3* (GenBank accession numbers: MG264424, MG264425 and MG264426) obtained were 975, 942 and 939 base pairs, which encoded 324, 313 and 312 amino acids. The predicted molecular weight/isoelectric point of TcPLR1, TcPLR2.2 and TcPLR3 were as follows: 36.4 kDa/5.82, 35.6 kDa/5.95 and 35.0 kDa/5.48. In the amino acid sequence of PLR, a conservative glycine-rich NAD(P)H-binding motif and a lysine residue are necessary for PLR activity. The glycine-rich motif bind with NADPH, and the lysine residue act as a general base to trigger proton transfer between NADPH and a substrate (Min et al. 2003). The conserved glycine-rich NAD(P)H-binding motif (GGXGXXG) and the lysine residue necessary for PLR catalytic activity could be observed in alignments of TcPLRs and other PLRs with different substrate enatiospecificity (Figure S4). The amino acid sequence between conifer PLRs (TcPLRs and TpPLRs from *T. plicata*) were compared (Table S5), which showed

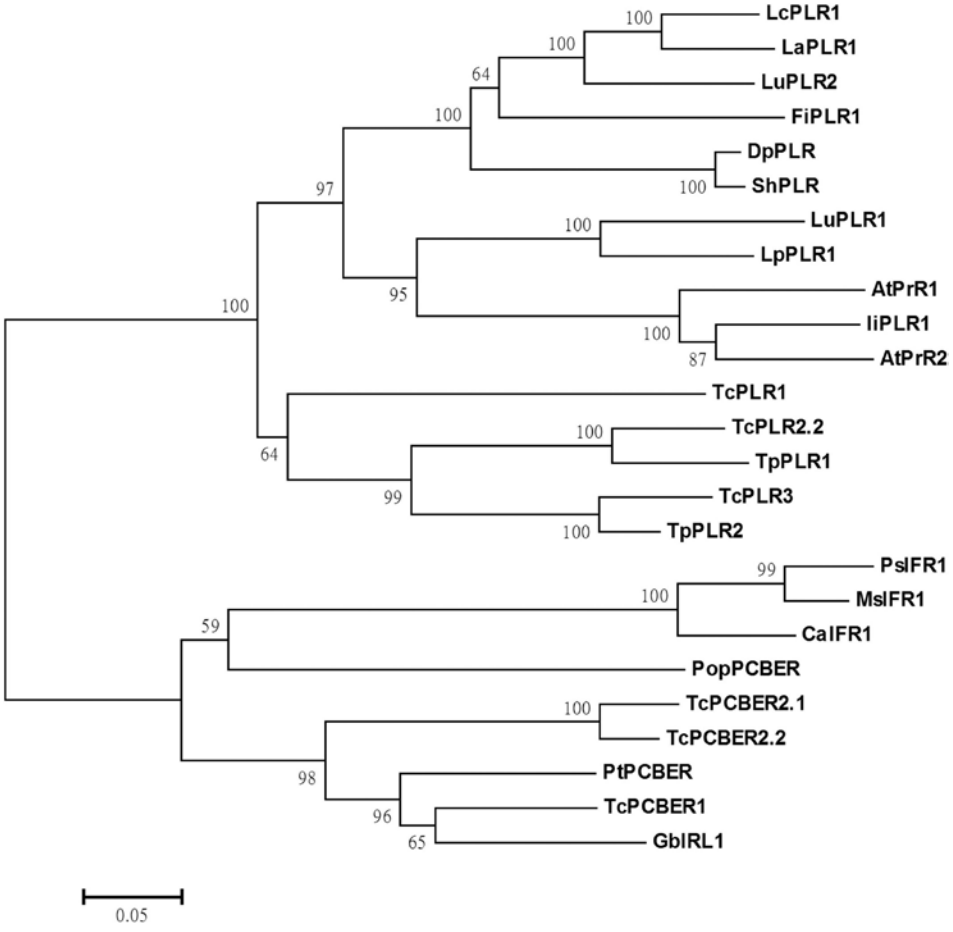

Figure 4: Phylogenetic tree of PLRs, PrRs, PCBERs and IFRs.
Abbreviations of plant species and accession numbers of amino acid sequences are as follows: At, *Arabidopsis thaliana*; AtPrR1, AAM20170.1; AtPrR2, AAO42400.1; Ca, *Cicer arietinum*; CaIFR1, CAA43167.1; Dp, *Dysosma pleiantha*; DpPLR, AHL21381.1; Fi, *Forsythia x intermedia*; FiPLR1, AAC49608.1; Gb, *Ginkgo biloba*; GbIRL1, AGG40646.1; Ii, *Isatis indigotica*; IiPLR1, AEA42007.1; La, *Linum album*; LaPLR1, CAH60857.1; Lc, *Linum corymbulosum*; LcPLR1, ABW86959.1; Lp, *Linum perenne*; LpPLR1, ABM68630.1; Lu, *Linum usitatissimum*; LuPLR1, CAH60858.1; LuPLR2, ABW24501.1; Ms, *Medicago sativa*; MsIFR, AAC48976.1; Pop, *Populus trichocarpa*; PopPCBER, CAA06706.1; Ps, *Pisum sativum*; PsIFR1, AAB31368.1; Pt, *Pinus taeda*; PtPCBER, AAF64173.2; Sh, *Sinopodophyllum hexandrum*; ShPLR, ACF71492.1; Tp, *Thuja plicata*; TpPLR1, AAF63507.1; TpPLR2, AAF63508.1. Abbreviations of enzymes: IFR, Isoflavone reductase; IRL, isoflavone reductase-like; PCBER, phenylcoumaran benzylic ether reductase; PLR, pinoresinol-lariciresinol reductase; PrR, pinoresinol reductase.

that TcPLR2.2 and TcPLR3 share the higher sequence identity (72%) compared to TcPLR1. TcPLR2.2 and TcPLR3 had higher sequence identities to TpPLR1 (88%) and TpPLR2 (91%), respectively. TcPLR1 showed lower identities (61~64%) to the other TcPLRs and TpPLRs. To confirm the functions of TcPLRs, *in vitro* enzyme assays were performed on (+)-pinoresinol.

The supernatant of the cell lysate containing TcPLRs, DpPLR or the protein expression vector was used in enzyme assays. In comparison to the high-performance liquid chromatography (HPLC) analysis result of reaction extracts of the negative control (Figure S6), the LC-MS analysis of reaction products of TcPLRs showed that both TcPLR2.2 and TcPLR3 were able to reduce (+)-pinoresinol to (+)-lariciresinol and then to (−)-secoisolariciresinol [the chiral properties of products were deduced from the carbon skeleton of (+)-pinoresinol]. On the contrary, TcPLR1 could only reduce (+)-pinoresinol to (+)-lariciresinol (Figures 3 and S5). The results indicated the involvement of TcPLRs in lignan biosynthesis, although the sequence identity of TcPLR1 was lower compared to other conifer PLRs.

Phylogenetic analysis of TcPLRs and the catalytic activity of TcPLRs

The phylogenetic relationship of PLRs and the two enzymes participating in other phenylpropanoids biosynthesis – PCBER (neolignans, Figure 1) and IFR (isoflavones) are shown in Figure 4. Because the sequence similarities between PLR, PCBER and IFR were reported previously (Gang et al. 1999b), the TcPCBERs of Taiwania searched by PtPCBER of loblolly pine (*P. taeda*) were also included in the phylogenetic tree. TcPCBER1, TcPCBER2.1 and TcPCBER2.2, which, respectively, had 79, 73 and 74% identities to the amino acid sequence of PtPCBER, and 54, 49 and 50% identities to TpPLR2, clustered together with other conifer PCBERs from loblolly pine and ginkgo (*Ginkgo biloba*) instead of TcPLRs. This suggests that TcPCBERs may participate in neolignan biosynthesis and that TcPLRs are more likely to participate in lignan biosynthesis, which is in agreement with our enzyme assay results. The poplar (*Populus trichocarpa*) PCBER clustered more closely with IFRs of chickpea (*Cicer arietinum* L.), alfalfa (*Medicago sativa* L.) and pea (*Pisum sativum* L.), which may be due to the angiosperm origin.

The PLR clade was first clustered according to the gymnosperm or angiosperm origin. In the angiosperm PLR clade, PLRs with similar substrate enantioselectivity clustered together in advance of taxonomic classification (Figures 1 and 4), as presented by the phylogenetic analysis in previous reports (von Heimendahl et al. 2005; Bayindir et al. 2008; Nakatsubo et al. 2008). In the gymnosperm PLR clade, the two PLRs of *T. plicata* separately clustered with TcPLR2.2 and TcPLR3. In our enzyme assay with (+)-pinoresinol as substrate, both TcPLR2.2 and TcPLR3 could catalyze the same reaction to produce (+)-lariciresinol and (−)-secoisolariciresinol. This can be interpreted that either the two TcPLRs exhibit the ablility to reduce (±)-pinoresinol and (+)-lariciresinol like TpPLR2, or does not exhibit substrate enantioselectivity toward pinoresinol and lariciresinol. TcPLR1, which clustered apart from other conifer PLRs, could reduce (+)-pinoresinol to (+)-lariciresinol but could not reduce (+)-lariciresinol to (−)-secoisolariciresinol. TcPLR1 may have the same catalytic activity as TpPLR1, which selectively reduces (−)-lariciresinol. Future studies on the catalytic activity of TcPLRs toward (−)-pinoresinol reduction, and the content ratio of lignan enantiomers in wood extractives would help in understanding lignan biosynthesis in Taiwania.

Conclusions

On the basis of the transcriptome of Taiwania, three *PLR*s (*TcPLR1*, *TcPLR2.2* and *TcPLR3*) were cloned and the complete ORFs were obtained. RNA-seq and RT-PCR results in wood tissues showed that *TcPLR*s had the highest expression levels in Cam and sW, which are probably the sites of biosynthesis of upstream lignans. Enzyme assays *in vitro* revealed that TcPLR2.2 and TcPLR3 had PLR activity, namely reducing (+)-pinoresinol to (+)-lariciresinol and next to (−)-secoisolariciresinol, while TcPLR1 only reduced (+)-pinoresinol to (+)-lariciresinol.

Author contributions: All the authors have accepted responsibility for the entire content of this submitted manuscript and approved submission.
Research funding: Financial assistance from the Ministry of Science and Technology of Taiwan is gratefully acknowledged.
Employment or leadership: None declared.
Honorarium: None declared.

References

Adlercreutz, H. (2007) Lignans and human health. Crit. Rev. Clin. Lab. Sci. 44:483–525.

Bayindir, Ü., Alfermann, A.W., Fuss, E. (2008) Hinokinin biosynthesis in *Linum corymbulosum* Reichenb. Plant J. 55:810–820.

Bergstrom, B. (2003) Chemical and structural changes during heartwood formation in *Pinus sylvestris*. Forestry 76:45–53.

Bolger, A.M., Lohse, M., Usadel, B. (2014) Trimmomatic: a flexible trimmer for Illumina sequence data. Bioinformatics 30:2114–2120.

Bugos, R.C., Chiang, V.L., Zhang, X.H., Campbell, E.R., Podila, G.K., Campbell, W.H. (1995) RNA isolation from plant tissues recalcitrant to extraction in guanidine. Biotechniques 19:734–737.

Burlat, V., Kwon, M., Davin, L.B., Lewis, N.G. (2001) Dirigent proteins and dirigent sites in lignifying tissues. Phytochemistry 57:883–897.

Celedon, J.M., Chiang, A., Yuen, M.M.S., Diaz-Chavez, M.L., Madilao, L.L., Finnegan, P.M., Barbour, E.L., Bohlmann, J. (2016) Heartwood-specific transcriptome and metabolite signatures of tropical sandalwood (*Santalum album*) reveal the final step of (*Z*)-santalol fragrance biosynthesis. Plant J. 86:289–299.

Chang, S., Puryear, J., Cairney, J. (1993) A simple and efficient method for isolating RNA from pine trees. Plant Mol. Biol. Rep. 11:113–116.

Chang, S.T., Wang, S.Y., Su, Y.C., Huang, S.L., Kuo, Y.H. (1999) Chemical constituents and mechanisms of discoloration of Taiwania (*Taiwania cryptomerioides* Hayata) heartwood – 1. The structure reconfirmation and conversion mechanism of taiwanin A. Holzforschung 53:142–146.

Chang, S.T., Wang, D.S.Y., Wu, C.L., Shiah, S.G., Kuo, Y.H., Chang, C.J. (2000) Cytotoxicity of extractives from *Taiwania cryptomerioides* heartwood. Phytochemistry 55:227–232.

Chang, S.T., Wang, S.Y., Kuo, Y.H. (2003) Resources and bioactive substances from Taiwania (*Taiwania cryptomerioides*). J. Wood Sci. 49:1–4.

Chen, R.B., Li, Q., Tan, H.X., Chen, J., Xiao, Y., Ma, R., Gao, S., Zerbe, P., Chen, W., Zhang, L. (2015) Gene-to-metabolite network for biosynthesis of lignans in MeJA-elicited *Isatis indigotica* hairy root cultures. Front. Plant Sci. 6:952.

Cheng, H., Li, L.L., Xu, F., Wang, Y., Yuan, H.H., Wu, C.H., Wang, S.B., Liao, Z.Q., Hua, J., Wang, Y.P., Cheng, S.Y., Cao, F.L. (2013) Expression patterns of an isoflavone reductase-like gene and its possible roles in secondary metabolism in *Ginkgo biloba*. Plant Cell Rep. 32:637–650.

Cheng, Q., Li, N., Dong, L., Zhang, D., Fan, S., Jiang, L., Wang, X., Xu, P., Zhang, S. (2015) Overexpression of soybean isoflavone reductase (GmIFR) enhances resistance to *Phytophthora sojae* in soybean. Front. Plant Sci. 6:1024.

Chien, S.C., Kuo, Y.H. (2009) Review of the chemical constitutes of *Taiwania cryptomerioides*. J. Chin. Chem. Soc. 67:33–44.

Chou, Y.W., Thomas, P.I., Ge, X.J., LePage, B.A., Wang, C.N. (2011) Refugia and phylogeography of *Taiwania* in East Asia. J. Biogeogr. 38:1992–2005.

Corbin, C., Drouet, S., Mateljak, I., Markulin, L., Decourtil, C., Renouard, S., Lopez, T., Doussot, J., Lamblin, F., Auguin, D., Laine, E., Fuss, E., Hano, C. (2017) Functional characterization of the pinoresinol-lariciresinol reductase-2 gene reveals its roles in yatein biosynthesis and flax defense response. Planta 246:405–420.

Dalisay, D.S., Kim, K.W., Lee, C., Yang, H., Rübel, O., Bowen, B.P., Davin, L.B., Lewis, N.G. (2015) Dirigent protein-mediated lignan and cyanogenic glucoside formation in flax seed: integrated omics and MALDI mass spectrometry imaging. J. Nat. Prod. 78:1231–1242.

Dinkova-Kostova, A.T., Gang, D.R., Davin, L.B., Bedgar, D.L., Chu, A., Lewis, N.G. (1996) (+)-Pinoresinol/(+)-lariciresinol reductase from *Forsythia intermedia*. Protein purification, cDNA cloning, heterologous expression and comparison to isoflavone reductase. J. Biol. Chem. 271:29473–29482.

Fauré, M., Lissi, E., Torres, R., Videla, L.A. (1990) Antioxidant activities of lignans and flavonoids. Phytochemistry 29:3773–3775.

Fujita, M., Gang, D.R., Davin, L.B., Lewis, N.G. (1999) Recombinant pinoresinol-lariciresinol reductases from western red cedar (*Thuja plicata*) catalyze opposite enantiospecific conversions. J. Biol. Chem. 274:618–627.

Gang, D.R., Costa, M.A., Fujita, M., Dinkova-Kostova, A.T., Wang, H.B., Burlat, V., Martin, W., Sarkanen, S., Davin, L.B., Lewis, N.G. (1999a) Regiochemical control of monolignol radical coupling: a new paradigm for lignin and lignan biosynthesis. Chem. Biol. 6:143–151.

Gang, D.R., Kasahara, H., Xia, Z.Q., Vander Mijnsbrugge, K., Bauw, G., Boerjan, W., Van Montagu, M., Davin, L.B., Lewis, N.G. (1999b) Evolution of plant defense mechanisms. Relationships of phenylcoumaran benzylic ether reductases to pinoresinol-lariciresinol and isoflavone reductases. J. Biol. Chem. 274:7516–7527.

Grabherr, M.G., Haas, B.J., Yassour, M., Levin, J.Z., Thompson, D.A., Amit, I., Adiconis, X., Fan, L., Raychowdhury, R., Zeng, Q.D., Chen, Z.H., Mauceli, E., Hacohen, N., Gnirke, A., Rhind, N., di Palma, F., Birren, B.W., Nusbaum, C., Lindblad-Toh, K., Friedman, N., Regev, A. (2011) Full-length transcriptome assembly from RNA-Seq data without a reference genome. Nat. Biotechnol. 29:644–652.

Harmatha, J., Dinan, L. (2003) Biological activities of lignans and stilbenoids associated with plant-insect chemical interactions. Phytochem. Rev. 2:321–330.

Harn, H.J., Chuang, H.M., Chang, L.F., Huang, A., Hsieh, S.T., Lin, S.Z., Chou, C.W., Kuo, Y.H., Chiou, T.W. (2014) Taiwanin A targets non-steroidal anti-inflammatory drug-activated gene-1 in human lung carcinoma. Fitoterapia 99:227–235.

Hemmati, S., Schmidt, T.J., Fuss, E. (2007) (+)-Pinoresinol/(–)-lariciresinol reductase from *Linum perenne* Himmelszelt involved in the biosynthesis of justicidin B. FEBS Lett. 581:603–610.

Hemmati, S., von Heimendahl, C.B.I., Klaes, M., Alfermann, A.W., Schmidt, T.J., Fuss, E. (2010) Pinoresinol-lariciresinol reductases with opposite enantiospecificity determine the enantiomeric composition of lignans in the different organs of *Linum usitatissimum* L. Planta Med. 76:928–934.

Ho, P.J., Chou, C.K., Kuo, Y.H., Tu, L.C., Yeh, S.F. (2007) Taiwanin A induced cell cycle arrest and p53-dependent apoptosis in human hepatocellular carcinoma HepG2 cells. Life Sci. 80:493–503.

Johansson, C.I., Saddler, J.N., Beatson, R.P. (2000) Characterization of the polyphenolics related to the colour of western red cedar (*Thuja plicata* Donn) heartwood. Holzforschung 54:246–254.

Kemp, M.S., Burden, R.S. (1986) Phytoalexins and stress metabolites in the sapwood of trees. Phytochemistry 25:1261–1269.

Kim, M.K., Jeon, J.H., Fujita, M., Davin, L.B., Lewis, N.G. (2002) The western red cedar (*Thuja plicata*) 8-8′ *DIRIGENT* family displays diverse expression patterns and conserved monolignol coupling specificity. Plant Mol. Biol. 49:199–214.

Kim, K.W., Moinuddin, S.G.A., Atwell, K.M., Costa, M.A., Davin, L.B., Lewis, N.G. (2012) Opposite stereoselectivities of dirigent proteins in *Arabidopsis* and *Schizandra* species. J. Biol. Chem. 287:33957–33972.

Kuo, H.J., Wei, Z.Y., Lu, P.C., Huang, P.L., Lee, K.T. (2014) Bioconversion of pinoresinol into matairesinol by use of recombinant *Escherichia coli*. Appl. Environ. Microbiol. 80:2687–2692.

Kwon, M., Davin, L.B., Lewis, N.G. (2001) In situ hybridization and immunolocalization of lignan reductases in woody tissues: implications for heartwood formation and other forms of vascular tissue preservation. Phytochemistry 57:899–914.

Larson, R.A. (1988) The antioxidants of higher-plants. Phytochemistry 27:969–978.

Lau, W., Sattely, E.S. (2015) Six enzymes from mayapple that complete the biosynthetic pathway to the etoposide aglycone. Science 349:1224–1228.

Lim, K.J., Paasela, T., Harju, A., Venäläinen, M., Paulin, L., Auvinen, P., Kärkkäinen, K., Teeri, T.H. (2016) Developmental changes in Scots pine transcriptome during heartwood formation. Plant Physiol. 172:1403–1417.

Liu, L.Y., Tseng, H.I., Lin, C.P., Lin, Y.Y., Huang, Y.H., Huang, C.K., Chang, T.H., Lin, S.S. (2014) High-throughput transcriptome analysis of the leafy flower transition of *Catharanthus roseus* induced by peanut witches'-broom phytoplasma infection. Plant Cell Physiol. 55:942–957.

Love, M.I., Huber, W., Anders, S. (2014) Moderated estimation of fold change and dispersion for RNA-seq data with DESeq2. Genome Biol. 15:550.

MacRae, W.D., Towers, G.H.N. (1984) Biological activities of lignans. Phytochemistry 23:1207–1220.

Magel, E.A. (2000) Biochemistry and physiology of heartwood formation. In: Cell and Molecular Biology of Wood Formation. Eds. Savidge, R., Barnett, J., Napier, R. BIOS Scientific Publishers, Oxford. pp. 363–376.

Min, T.P., Kasahara, H., Bedgar, D.L., Youn, B.Y., Lawrence, P.K., Gang, D.R., Halls, S.C., Park, H.J., Hilsenbeck, J.L., Davin, L.B., Lewis, N.G., Kang, C. (2003) Crystal structures of pinoresinol-lariciresinol and phenylcoumaran benzylic ether reductases and their relationship to isoflavone reductases. J. Biol. Chem. 278:50714–50723.

Nakaba, S., Arakawa, I., Morimoto, H., Nakada, R., Bito, N., Imai, T., Funada, R. (2016) Agatharesinol biosynthesis-related changes of ray parenchyma in sapwood sticks of *Cryptomeria japonica* during cell death. Planta 243:1225–1236.

Nakatsubo, T., Mizutani, M., Suzuki, S., Hattori, T., Umezawa, T. (2008) Characterization of *Arabidopsis thaliana* pinoresinol reductase, a new type of enzyme involved in lignan biosynthesis. J. Biol. Chem. 283:15550–15557.

Niculaes, C., Morreel, K., Kim, H., Lu, F.C., Mckee, L.S., Ivens, B., Haustraete, J., Vanholme, B., De Rycke, R., Hertzberg, M., Fromm, J., Bulone, V., Polle, A., Ralph, J., Boerjan, W. (2014) Phenylcoumaran benzylic ether reductase prevents accumulation of compounds formed under oxidative conditions in poplar xylem. Plant Cell. 26:3775–3791.

Nuoendagula, Kamimura, N., Mori, T., Nakabayashi, R., Tsuji, Y., Hishiyama, S., Saito, K., Masai, E., Kajita, S. (2016) Expression and functional analyses of a putative phenylcoumaran benzylic ether reductase in *Arabidopsis thaliana*. Plant Cell Rep. 35:513–526.

Paiva, N.L., Edwards, R., Sun, Y.J., Hrazdina, G., Dixon, R.A. (1991) Stress responses in alfalfa (*Medicago sativa* L.) 11. Molecular cloning and expression of alfalfa isoflavone reductase, a key enzyme of isoflavonoid phytoalexin biosynthesis. Plant Mol. Biol. 17:653–667.

Paiva, N.L., Sun, Y.J., Dixon, R.A., Vanetten, H.D., Hrazdina, G. (1994) Molecular cloning of isoflavone reductase from pea (*Pisum sativum* L): evidence for a 3*R*-isoflavanone intermediate in (+)-pisatin biosynthesis. Arch. Biochem. Biophys. 312:501–510.

Patten, A.M., Davin, L.B., Lewis, N.G. (2008) Relationship of dirigent protein and 18s RNA transcript localization to heartwood formation in western red cedar. Phytochemistry 69:3032–3037.

Pittermann, J., Stuart, S.A., Dawson, T.E., Moreau, A. (2012) Cenozoic climate change shaped the evolutionary ecophysiology of the Cupressaceae conifers. Proc. Natl. Acad. Sci. USA 109:9647–9652.

Roberts, A., Pachter, L. (2013) Streaming fragment assignment for real-time analysis of sequencing experiments. Nat. Methods 10:71–73.

Saguez, J., Attoumbré, J., Giordanengo, P., Baltora-Rosset, S. (2013) Biological activities of lignans and neolignans on the aphid *Myzus persicae* (Sulzer). Arthropod Plant Interact. 7:225–233.

Satake, H., Koyama, T., Bahabadi, S.E., Matsumoto, E., Ono, E., Murata, J. (2015) Essences in metabolic engineering of lignan biosynthesis. Metabolites 5:270–290.

Shyur, L.F., Lee, S.H., Chang, S.T., Lo, C.P., Kuo, Y.H., Wang, S.Y. (2010) Taiwanin A inhibits MCF-7 cancer cell activity through induction of oxidative stress, upregulation of DNA damage checkpoint kinases, and activation of p53 and FasL/Fas signaling pathways. Phytomedicine 18:16–24.

Suzuki, S., Umezawa, T. (2007) Biosynthesis of lignans and norlignans. J. Wood Sci. 53:273–284.

Suzuki, S., Umezawa, T., Shimada, M. (2002) Stereochemical diversity in lignan biosynthesis of *Arctium lappa* L. Biosci. Biotechnol. Biochem. 66:1262–1269.

Tamura, K., Stecher, G., Peterson, D., Filipski, A., Kumar, S. (2013) MEGA6: molecular evolutionary genetics analysis version 6.0. Mol. Biol. Evol. 30:2725–2729.

Tiemann, K., Inzé, D., Vanmontagu, M., Barz, W. (1991) Pterocarpan phytoalexin biosynthesis in elicitor-challenged chickpea (*Cicer arietinum* L) cell cultures. Purification, characterization and cDNA cloning of NADPH:isoflavone oxidoreductase. Eur. J. Biochem. 200:751–757.

Tsao, N.W., Sun, Y.H., Chien, S.C., Chu, F.H., Chang, S.T., Kuo, Y.H., Wang, S.Y. (2016) Content and distribution of lignans in *Taiwania cryptomerioides* Hayata. Holzforschung 70:511–518.

Vanholme, R., Demedts, B., Morreel, K., Ralph, J., Boerjan, W. (2010) Lignin biosynthesis and structure. Plant Physiol. 153:895–905.

Vargas-Arispuro, I., Reyes-Báez, R., Rivera-Castañeda, G., Martínez-Téllez, M.A., Rivero-Espejel, I. (2005) Antifungal lignans from the creosotebush (*Larrea tridentata*). Ind. Crop. Prod. 22:101–107.

Vassão, D.G., Kim, K.W., Davin, L.B., Lewis, N.G. (2010) 1.23 – Lignans (neolignans) and allyl/propenyl phenols: biogenesis, structural biology, and biological/human health considerations. In: Comprehensive Natural Products II. Eds. Liu, H.W., Mander, L. Elsevier, Oxford. pp. 815–928.

von Heimendahl, C.B.I., Schäfer, K.M., Eklund, P., Sjöholm, R., Schmidt, T.J., Fuss, E. (2005) Pinoresinol-lariciresinol reductases with different stereospecificity from *Linum album* and *Linum usitatissimum*. Phytochemistry 66:1254–1263.

Xia, Z.Q., Costa, M.A., Pélissier, H.C., Davin, L.B., Lewis, N.G. (2001) Secoisolariciresinol dehydrogenase purification, cloning, and functional expression. Implications for human health protection. J. Biol. Chem. 276:12614–12623.

Xiao, Y., Ji, Q., Gao, S.H., Tan, H.X., Chen, R.B., Li, Q., Chen, J.F., Yang, Y.B., Zhang, L., Wang, Z.T., Chen, W.S., Hu, Z.B. (2015) Combined transcriptome and metabolite profiling reveals that *Ii*PLR1 plays an important role in lariciresinol accumulation in *Isatis indigotica*. J. Exp. Bot. 66:6259–6271.

Yoshida, K., Nishiguchi, M., Futamura, N., Nanjo, T. (2007) Expressed sequence tags from *Cryptomeria japonica* sapwood during the drying process. Tree Physiol. 27:1–9.

Zhao, Q., Zeng, Y.N., Yin, Y.B., Pu, Y.Q., Jackson, L.A., Engle, N.L., Martin, M.Z., Tschaplinski, T.J., Ding, S.Y., Ragauskas, A.J., Dixon, R.A. (2015) Pinoresinol reductase 1 impacts lignin distribution during secondary cell wall biosynthesis in *Arabidopsis*. Phytochemistry 112:170–178.

Zheng, P.M., Aoki, D., Yoshida, M., Matsushita, Y., Imai, T., Fukushima, K. (2014) Lignification of ray parenchyma cells in the xylem of *Pinus densiflora*. Part I: microscopic investigation by POM, UV microscopy, and TOF-SIMS. Holzforschung 68:897–905.

Supplementary Material: The online version of this article offers supplementary material (https://doi.org/10.1515/hf-2018-0026).